[2]W. E. Bron, Phys. Rev. 185, 1163 (1969).
[3]W. E. Bron and Max Wagner, Phys. Rev. 167, 841 (1968).
[4]Max Wagner, Z. Physik 214, 78 (1968).
[5]M. Buchanan and E. J. Woll, Jr., Can. J. Phys. 47, 1757 (1969).
[6]J. B. Page, Jr. and B. G. Dick, Phys. Rev. 163, 910 (1967).
[7]J. B. Page, Jr. and D. Strauch, Phys. Status Solidi 24, 469 (1967).
[8]M. J. L. Sangster and C. W. McCombie, J. Phys. C 3, 1498 (1970).
[9]J. E. Ralph and M. G. Townsend, J. Chem. Phys. 48, 149 (1968).
[10]J. E. Ralph and M. G. Townsend, J. Phys. C 3, 8 (1970).
[11]M. D. Sturge, Phys. Rev. 130, 639 (1963).
[12]G. F. Imbusch, M. L. Report No. 1190, Stanford University, 1964 (unpublished).
[13]A. M. Glass and T. M. Searle, J. Chem. Phys. 46, 2092 (1967).
[14]G. Peckham, Proc. Phys. Soc. (London) 90, 657 (1967).
[15]R. J. Buckland and D. H. Saunderson, Atomic Energy Research Establishment, Harwell, Report No. R-5467, 1967 (unpublished).
[16]R. E. Watson and A. J. Freeman, Phys. Rev. 134, A1526 (1964); S. Sugano and R. G. Shulman, *ibid.* 130, 517 (1963).
[17]N. B. Manson, following Paper, Phys. Rev. B 4, 2656 (1971).
[18]R. Pappalardo, D. L. Wood, and R. C. Linares, J. Chem. Phys. 35, 1460 (1961).
[19]W. Low, Phys. Rev. 109, 247 (1958).
[20]N. B. Manson, Ph. D. thesis (University of Aberdeen, 1968) (unpublished).
[21]H. A. Jahn and E. Teller, Proc. Roy. Soc. (London) A161, 220 (1937).
[22]J. E. Wertz, J. W. Orton, and P. Auzins, J. Appl. Phys. Suppl. 33, 322 (1962).
[23]The shell and core displacements between 0 and 500 cm^{-1} are not significantly different and hence the core-core, core-shell, and shell-shell Green's functions are similar. Above 500 cm^{-1} the negative-ion's shell displacements are typically half that of its core, but there is only little intensity in this region without any pronounced features and, therefore, it does not destroy the over-all similarity between the core and shell Green's functions.
[24]A. G. Shenstone, J. Opt. Soc. Am. 44, 749 (1954).
[25]S. Koide and M. H. L. Pryce, Phil. Mag. 3, 607 (1958).
[26]A. D. Liehr and C. J. Ballhausen, Ann. Phys. (N. Y.) 6, 134 (1959).

PHYSICAL REVIEW B VOLUME 4, NUMBER 8 15 OCTOBER 1971

Multiphonon Vibronic Transition $^1T_{2g}$-$^3A_{2g}$ of Ni^{2+} in MgO†

N. B. Manson*
Department of Physics, University of California, Los Angeles, California 90024
(Received 1 June 1970)

The $\Gamma_{5g}(^1T_{2g}, t_{2g}^5 e_g^3)$-$\Gamma_{5g}(^3A_{2g}, t_{2g}^6 e_g^2)$ vibronic spectrum is recorded in absorption and emission—under x-ray excitation—at crystal temperatures of 77 and 5 °K. The spectrum involves up to four phonon processes and a theoretical treatment of such a transition is presented. A possible explanation of the band is suggested and, by using imperfect-lattice Green's functions for the nearest-neighbor motion, it is constructed to give excellent agreement with experiment. The transition is forced (electric dipole) by one of the T_{1u} vibrations of the nearest-neighbor complex. Additional E_g vibrations couple in the higher phonon processes which suggest the presence of a Jahn-Teller distortion in the $^1T_{2g}$ excited state. However, it has not been possible to establish the presence of such a Jahn-Teller distortion from any other experimental data. A similar calculation is undertaken for the two-phonon band of the $\Gamma_{3g}(^3T_{2g}, t_{2g}^5, e_g^3)$-$\Gamma_{5g}(^3A_{2g}, t_{2g}^6 e_g^2)$ transition of Ni^{2+} in MgO. Again there is an indication of a coupling to E_g vibrations in the two-phonon process.

I. INTRODUCTION

In Paper I[1] the vibronic band associated with the single electronic transition $\Gamma_{3g}(^3T_{2g}, t_{2g}^5 e_g^3)$-$\Gamma_{5g}$ $(^3A_{2g}, t_{2g}^6 e_g^2)$ of MgO:Ni^{2+} is studied and good agreement is obtained between the one-phonon structure and that predicted by a Green's-function treatment of the motion of the impurity ion and its six nearest neighbors. In this paper the calculations are extended to consider higher-order phonon processes; the main focus of attention being $\Gamma_{5g}(^1T_{2g}, t_{2g}^5 e_g^3)$-$\Gamma_{5g}(^3A_{2g}, t_{2g}^6 e_g^2)$ vibronic transitions in MgO:Ni^{2+}. In this case both states are well isolated from other electronic levels and the vibronic band associated with this single electronic transition is seen very clearly in emission, weakly in absorption. A possible construction of the band is proposed. It is constructed with localized Green's functions using semiempirical parameters and compared to the observed band. A similar treatment for the two-phonon sideband of the $\Gamma_{3g} \rightarrow \Gamma_{5g}$ is presented and a comparison made between the

two cases.

In Paper I, a simple but crude model was used successfully to predict the one-phonon coupling parameters. This calculation is repeated here for the $\Gamma_{3g} \rightarrow \Gamma_{5g}$ transition and the results briefly discussed.

II. EXPERIMENT

A synopsis of the MgO : Ni^{2+} spectrum is given in Paper I. The spin-forbidden transition between the ground state $\Gamma_{5g}(^3A_{2g}, t_{2g}^6 e_g^2)$ and the $\Gamma_{5g}(^1T_{2g}, t_{2g}^5 e_g^3)$ state is seen in both absorption and emission. These have been reported by Ralph and Townsend.[2,3] Here the emission spectrum is reported in higher resolution, although less structure is seen. The band can be excited by x rays (15 mA, 55 kV) or electron beam and is then two orders of magnitude more intense than by the use of optical lamps available in the laboratory. Details of the x-ray stimulation are as follows:

A 1-kW x-ray tube with a tungsten target was used. The effective focus of the beam was an area 1×1 mm which lay 7.5 cm vertically below the position of the crystal sample in the helium Dewar. The x rays pass through two windows: one a window on the x-ray-tube head and a 1-μ-thick platelet of mica which replaces the bottom window of the helium Dewar. The x-ray set was normally run at 55 kV and a beam current of 15 mA, but other settings at the same power gave only minor changes (~ 10%) of the fluorescence intensity. The light emitted from the sample at right angles was analysed by a Hilger and Watts prism spectrometer using spectral slit width of 7 cm^{-1} and detected by an EMI 9558 photomultiplier.

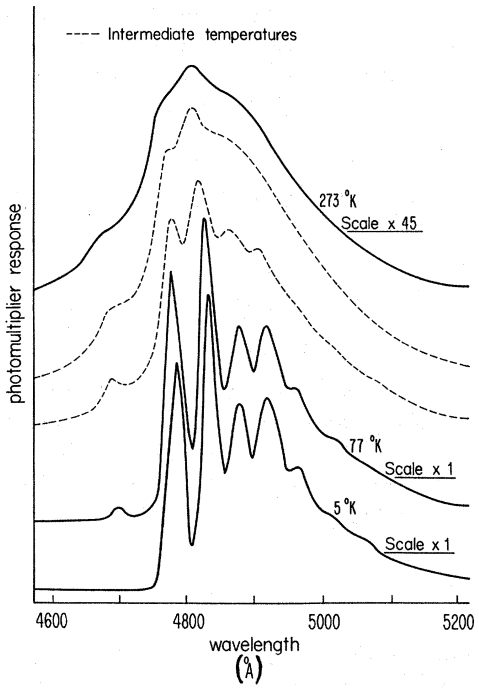

FIG. 1. MgO : Ni^{2+}. 20 000-cm^{-1} emission band for various temperatures.

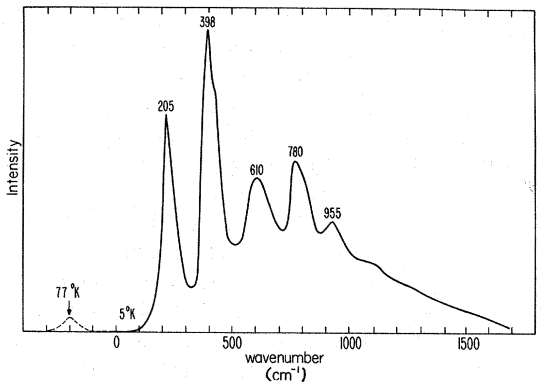

FIG. 2. $\Gamma_{5g}(^1T_{2g}, t_{2g}^5 e_g^3)$-$\Gamma_{5g}(^3A_{2g}, t_{2g}^6 e_g^2)$ emission band at helium temperature corrected for system response. The electronic origin lies at 21 095 cm^{-1} and the horizontal scale gives displacements from this position.

The crystal was clamped to the cooled copper finger of a helium Dewar, and its temperature was measured using a copper-constantan thermocouple with the junction firmly clamped to the side of the crystal.

III. EXPERIMENTAL RESULTS

The fluorescence has been recorded at several temperatures between room and liquid helium. These are indicated in Fig. 1, and Fig. 2 gives the trace at helium temperature corrected for system response.

The small peak at 21 300 cm^{-1} which appears at nitrogen temperatures and above must arise from population of an excited level (either electronic or vibrational) via the Boltzman distribution factor. If this peak corresponds to the annihilation of a phonon corresponding to the phonon creation peak at 20 890 cm^{-1} (i.e., a 205-cm^{-1} vibrational peak), the ratio of its peak intensity to that at 20 890 cm^{-1} should equal $e^{-hc\Delta E/kT}$ with $\Delta E = 205$ cm^{-1}. The ratio of their intensities is measured for various temperatures between 50 and 200 °K and found to correspond to a $\Delta E = 195 \pm 15$ cm^{-1}, in favorable agreement with that expected. The emission band is thus considered to be the vibronic transition from a single or very closely spaced set of electronic levels at 21 095 cm^{-1}.

The excited state involved is the $^1T_{2g}(t_{2g}^5 e_g^3)$ predicted by Liehr and Ballhausen[4] using parameters $F_2 = 1400$ cm^{-1}, $Dq = -830$ cm^{-1}, and $\lambda = -325$ cm^{-1} to lie at 21 350 cm^{-1}. This state may be split by the Jahn-Teller[5] effect, but there is no direct

optical evidence of any lifting of the degeneracy with only a small sharpening of the spectrum on approaching helium temperatures.

At first inspection it would appear that there is a progression of 200 cm^{-1}.[6] However, both the exact intervals and the slight irregularity in the intensity distribution suggests that this is unlikely. Furthermore, the transition is forced electric dipole and therefore the first phonon process must have odd parity. Higher-order processes on the other hand are more probably of even parity. Certainly, in the two-phonon process one must be odd and the second one even. When there is an odd number of phonons involved, it is possible for further odd-parity vibrations to couple in pairs, but coupling of even ones is generally stronger. The first two peaks in the observed spectrum are both within the range of lattice vibrations of MgO and correspond well to peaks in the Green's functions for the $T_{1u}^{(1)}$ odd-symmetry displacements for a Ni^{2+} substituted lattice with small negative force-constant changes (see Ref. 1, Fig. 6). The intensity ratio and the separation of the first and second peaks is repeated for the third and fourth implying that there is a coupling to a phonon distribution with a peak at 400 cm^{-1}—a value (as it will be shown later) in close agreement with the E_g (or T_{1g}) Green's function. Repeated coupling to this even phonon distribution would then give rise to the rest of the band. A detailed calculation and a theoretical treatment of processes involving two and more phonons is employed to justify this interpretation.

IV. THEORY

The Hamiltonian for the d^8 configuration in a cubic crystal field is taken as

$$\mathcal{H}=\mathcal{H}_{\text{free ion}}+\mathcal{H}_{\text{cubic}}+\mathcal{H}_{LS} \quad . \tag{1}$$

The perturbation giving rise to the vibronic band is given by $\mathcal{H}'=P+V$, where P is the interaction of the Ni^{2+} electrons with the photon field, and V is the electron-phonon interaction. The interaction potential V expanded in a power series of the lattice displacements (from the equilibrium position of the defect lattice) is given by

$$\begin{aligned} V(\vec{r},X) &= V_1(\vec{r},X)+V_2(\vec{r},X)+\cdots \\ &= \sum_{\Gamma\gamma n} V_{\Gamma\gamma}^{(n)}(\vec{r})X_{\Gamma\gamma}^{(n)} \\ &\quad + \frac{1}{2!}\sum_{\substack{\Gamma\gamma n\\ \Gamma'\gamma' n'}} V_{\Gamma\gamma,\Gamma'\gamma'}^{(nn')}(\vec{r})X_{\Gamma\gamma}^{(n)}X_{\Gamma'\gamma'}^{(n')}+\cdots , \end{aligned} \tag{2}$$

where the symmetry displacements $X_{\Gamma\gamma}^{(n)}$ (of the impurity ion and six nearest O^{-2} ions) and the electron coupling functions $V_{\Gamma\gamma}^{(n)}$ each transform as the irreducible representation Γ, row $\gamma-n$ being used to distinguish between displacements of the same symmetry. V_r used in Eq. (2) is the term in the interaction potential containing displacements to the degree r. The electronic coupling functions $V_{\Gamma\gamma}^{(n)}(\vec{r})$ and $V_{\Gamma\gamma,\Gamma'\gamma'}^{(nn')}(\vec{r})$ are derivatives of the electron potential evaluated at the equilibrium configuration of the imperfect lattice.

A. One-Phonon Coupling

In the notation introduced in Ref. 1 the probability of one-phonon creation in the low-temperature limit when going from electronic level e to the final electronic state f is given by

$$W_{e\to f}=\frac{2\pi}{\hbar}\sum_{\gamma_e\gamma_f}\sum_{\text{final states}}\left|\sum_{\Gamma_i\gamma_i a_i}\left\{\frac{\langle 1\chi_1\Gamma_f\gamma_f|P|0\chi_1 a_i\Gamma_i\gamma_i\rangle\langle 0\chi_1 a_i\Gamma_i\gamma_i|V_1|0\chi_0\Gamma_e\gamma_e\rangle}{\mathcal{E}_i-\mathcal{E}_e+\hbar\omega}\right.\right.$$
$$\left.\left.+\frac{\langle 1\chi_1\Gamma_f\gamma_f|V_1|1\chi_0 a_i\Gamma_i\gamma_i\rangle\langle 1\chi_0 a_i\Gamma_i\gamma_i|P|0\chi_0\Gamma_e\gamma_e\rangle}{\mathcal{E}_i-\mathcal{E}_f-\hbar\omega}\right\}\right|^2\delta(\mathcal{E}_f-\mathcal{E}_e+\hbar\nu+\hbar\omega) \quad . \tag{3}$$

The total wave function is written $|n\chi_h a_k\Gamma_k\gamma_k\rangle$. n denotes the number of photons; $\chi_h(\vec{k},j)$ is the harmonic oscillator wave function of the $\vec{k},j$ mode ($\vec{k},j$ omitted for brevity), all other oscillators being in their zeroth occupational state; and $|a_k\Gamma_k\gamma_k\rangle$ is the electronic wave function belonging to the irreducible representation Γ_k, row γ_k-a_k being used to distinguish between states of same symmetry but is dropped for the initial $|\Gamma_e\gamma_e\rangle$ and final $|\Gamma_f\gamma_f\rangle$ states. The energies of the phonon, associated photon, initial, intermediate, and final electronic states are given by $\hbar\omega$, $\hbar\nu$, $\mathcal{E}_f$, $\mathcal{E}_i$, and $\mathcal{E}_e$, respectively. The initial and final electronic states are both of even parity and hence the transition is only permitted by the odd-parity components of the interaction—coupling odd-parity intermediate electronic states. The states lie considerably above the d^8 levels such that

$$\hbar\omega \ll (\mathcal{E}_i-\mathcal{E}_f)\simeq(\mathcal{E}_i-\mathcal{E}_e) \quad , \tag{4}$$

and will be neglected in the energy denominators. The transition rate for light polarized in the y direction, with angular frequency between ν and $\nu+\Delta\nu(\Delta\nu=\Delta\omega)$ observed in solid angle $\Delta\Omega$ is then

$$W_{e\to f} = W^{(1)}(\omega)\Delta\omega = \frac{\Delta\Omega\Delta\omega\nu^3 e^2}{2\pi c^3}$$

$$\times \sum_{\Gamma nn'} \left(\sum_{\gamma} \sum_{\gamma_e \gamma_f} F^{\gamma_e\to\gamma_f}_{y\Gamma\gamma n} F^{\gamma_e\to\gamma_f *}_{y\Gamma\gamma n'} \right) \mathrm{Im}G^{(nn')}_{\Gamma}(\omega), \tag{5}$$

where

$$F^{\gamma_e\to\gamma_f}_{y\Gamma\gamma n} = \sum_{\Gamma_i\gamma_i a_i} \left(\frac{\langle \Gamma_f\gamma_f | y | a_i\Gamma_i\gamma_i\rangle \langle a_i\Gamma_i\gamma_i | V^{(n)}_{\Gamma\gamma} | \Gamma_e\gamma_e\rangle}{\mathcal{E}_i - \mathcal{E}_e} + \frac{\langle \Gamma_f\gamma_f | V^{(n)}_{\Gamma\gamma} | a_i\Gamma_i\gamma_i\rangle \langle a_i\Gamma_i\gamma_i | y | \Gamma_e\gamma_e\rangle}{\mathcal{E}_i - \mathcal{E}_f} \right), \tag{6}$$

and $\mathrm{Im}G^{(nn')}_{\Gamma}(\omega)$ is the imaginary part of the Green's function $G^{(nn')}_{\Gamma}(\omega)$ defined in Ref. 1.

B. Multiphonon Coupling

A two-phonon sideband arises from terms to the second power in lattice displacements; the linear term of Eq. (1) in second order or the quadratic term in first. These terms also give rise to a change in the lattice frequency between the two electronic states. However, because the absorption and emission exhibit similar vibrational frequencies (see Ref. 2), this must be small and will be neglected at present.

It is anticipated that for the second phonon process either the terms V_1 or V_2 will predominate. If the former is the case, then for the r-phonon process, V_1 will still give the larger contribution (type I); if the latter, then V_r (type II). Thus the two limiting cases are considered.

1. *Type* I: *Two Phonon*

The predominance of the linear term will later be taken to imply a presence of a Jahn-Teller-type distortion. It may appear that taking the Jahn-Teller interaction as a perturbation, whereas spin-orbit interaction is included in the original Hamiltonian, is being inconsistent. However, the off-diagonal terms of the Jahn-Teller interaction, apparently neglected, may be considered to be present as the coupling parameters are being treated empirically. Likewise, the spin-orbit coupling parameter is empirical and thus any change due to reduction of orbital momentum can be allowed for by adjusting this parameter. Note that the important contribution of the spin-orbit interaction is to mix terms of different multiplicity, thus permitting the "spin-forbidden" transitions. If this interaction is not included in the Hamiltonian, it would have to be included as a further perturbation, giving an even more complex form of the transition probability but without altering the final expressions in functional form.

The wave functions are still taken to be Born-Oppenheimer products even in the presence of the Jahn-Teller distortion. This will be justified later for the individual case considered.

The transition probability of a two-phonon process arising from terms linear in lattice displacement is given by third-order perturbation theory by

$$W_{e\to f} = \frac{2\pi}{\hbar} \sum_{\substack{\text{initial}\\ \text{and}\\ \text{final}\\ \text{states}}} \left| \sum_{il} \frac{\langle \Psi_f | P + V_1 | \Psi_i\rangle \langle \Psi_i | P + V_1 | \Psi_l\rangle \langle \Psi_l | P + V_1 | \Psi_e\rangle}{(E_i - E_e)\,(E_l - E_e)} \right|^2, \tag{7}$$

where V_1 is the first term in the expansion in Eq. (2). Ψ_k and E_k are the total wave function and total energy of the system in state k. Expanding this gives

$$W_{e\to f} = \frac{2\pi}{\hbar}$$

$$\times \sum_{\gamma_e\gamma_f} \sum_{\substack{\text{final}\\ \text{states}}} \left| \sum_{\Gamma_i\gamma_i a_i} \left(\frac{\langle 1\chi_1\chi_1'\Gamma_f\gamma_f | P | 0\chi_1\chi_1' a_i\Gamma_i\gamma_i\rangle \langle 0\chi_1\chi_1' a_i\Gamma_i\gamma_i | V_1 | 0\chi_0\chi_1' a_l\Gamma_l\gamma_l\rangle \langle 0\chi_0\chi_1' a_l\Gamma_l\gamma_l | V_1 | 0\chi_0\chi_0'\Gamma_e\gamma_e\rangle}{(\mathcal{E}_i - \mathcal{E}_e + \hbar\omega + \hbar\omega')(\mathcal{E}_l - \mathcal{E}_f + \hbar\omega')} \right.\right.$$

$$+ \frac{\langle 1\chi_1\chi_1'\Gamma_f\gamma_f | V_1 | 1\chi_1\chi_0' a_i\Gamma_i\gamma_i\rangle \langle 1\chi_1\chi_0' a_i\Gamma_i\gamma_i | P | 0\chi_1\chi_0' a_l\Gamma_l\gamma_l\rangle \langle 0\chi_1\chi_0' a_l\Gamma_l\gamma_l | V_1 | 0\chi_0\chi_0'\Gamma_e\gamma_e\rangle}{(\mathcal{E}_i - \mathcal{E}_f - \hbar\omega')(\mathcal{E}_l - \mathcal{E}_f + \hbar\omega)}$$

$$\left.\left. + \frac{\langle 1\chi_1\chi_1\Gamma_f\gamma_f | V_1 | 1\chi_0\chi_1' a_i\Gamma_i\gamma_i\rangle \langle 1\chi_0\chi_1' a_i\Gamma_i\gamma_i | V_1 | 1\chi_0\chi_0' a_l\Gamma_l\gamma_l\rangle \langle 1\chi_0\chi_0' a_l\Gamma_l\gamma_l | P | 0\chi_0\chi_0'\Gamma_e\gamma_e\rangle}{(\mathcal{E}_i - \mathcal{E}_f - \hbar\omega')(\mathcal{E}_l - \mathcal{E}_f - \hbar\omega - \hbar\omega')} \right) \right|^2 \delta(\mathcal{E}_f - \mathcal{E}_e + \hbar\nu + \hbar\omega + \hbar\omega') \tag{8}$$

where χ_h and $\chi_{h'}'$ represent $\chi_h(\vec{k}, j)$ and $\chi_{h'}(\vec{k}', j')$—the harmonic-oscillator wave function of the $(\vec{k}, j)$ and $(\vec{k}', j')$ mode in occupation state h and h', respectively, with all others being in their zeroth occupation state. Likewise ω and ω' represent $\omega(\vec{k}, j)$ and $\omega(\vec{k}', j')$. Note this expression (8) is not formulated correctly to cover the case $\vec{k}' = \vec{k}$, $j' = j$. However, it gives the same answer in the low-temperature limit and differs only by a negligible amount above 0 °K.

The wave functions of radiation field, vibrations or pure electronic, take on either even or odd parity but the total wave function maintains even parity. By keeping track of the changes in parity of the component functions the transition probability will be expressed more specifically. First, the linear perturbation in (2) is rewritten

$$V_1 = \sum_{\Gamma_u \gamma_u n} V^{(n)}_{\Gamma_u \gamma_u} X^{(n)}_{\Gamma_u \gamma_u} + \sum_{\Gamma_g \gamma_g} V_{\Gamma_g \gamma_g} X_{\Gamma_g \gamma_g} \quad , \tag{9}$$

where the first summation is restricted to odd displacement u and the second to even displacement g. In the XY_6 complex there is only one displacement of each of the even representations and, therefore, no (n) is included in the second term. Also u or g is included as suffix on the electronic wave functions to denote odd or even parity. The transition probability is then

$$W^{(2)}_{e\to f} = \frac{2\pi}{\hbar} \sum_{\gamma_e \gamma_f} \sum_{\substack{\text{final} \\ \text{states}}} \Bigg| \sum_{\substack{\Gamma_u \gamma_u n \\ \Gamma_g \gamma_g}} \sum_{\Gamma_{(ug)i} \gamma_i a_i}$$

$$\frac{\langle 1\chi_1\chi_1'\Gamma_{gf}\gamma_f | P | 0\chi_1\chi_1' a_i \Gamma_{ui}\gamma_i\rangle \langle 0\chi_1\chi_1' a_i \Gamma_{ui}\gamma_i | V^{(n)}_{\Gamma_u\gamma_u} X^{(n)}_{\Gamma_u\gamma_u} | 0\chi_0\chi_1' a_l \Gamma_{gl}\gamma_l\rangle \langle 0\chi_0\chi_1' a_l \Gamma_{gl}\gamma_l | V_{\Gamma_g\gamma_g} X_{\Gamma_g\gamma_g} | 0\chi_0\chi_0' \Gamma_{ge}\gamma_e\rangle}{(\mathcal{E}_{ui} - \mathcal{E}_e + \hbar\omega + \hbar\omega')(\mathcal{E}_{gl} - \mathcal{E}_e + \hbar\omega')}$$

$$+ \frac{\langle 1\chi_1\chi_1'\Gamma_{gf}\gamma_f | P | 0\chi_1\chi_1' a_i \Gamma_{ui}\gamma_i\rangle \langle 0\chi_1\chi_1' a_i \Gamma_{ui}\gamma_i | V_{\Gamma_g\gamma_g} X_{\Gamma_g\gamma_g} | 0\chi_1\chi_0' a_l \Gamma_{ul}\gamma_l\rangle \langle 0\chi_1\chi_0' a_l \Gamma_{ul}\gamma_l | V^{(n)}_{\Gamma_u\gamma_u} X^{(n)}_{\Gamma_u\gamma_u} | 0\chi_0\chi_0' \Gamma_{ge}\gamma_e\rangle}{(\mathcal{E}_{ui} - \mathcal{E}_e + \hbar\omega + \hbar\omega')(\mathcal{E}_{ul} - \mathcal{E}_e + \hbar\omega)}$$

$$+ \frac{\langle 1\chi_1\chi_1'\Gamma_{gf}\gamma_f | V^{(n)}_{\Gamma_u\gamma_u} X^{(n)}_{\Gamma_u\gamma_u} | 1\chi_0\chi_1' a_i \Gamma_{ui}\gamma_i\rangle \langle 1\chi_0\chi_1' a_i \Gamma_{ui}\gamma_i | P | 0\chi_0\chi_1' a_l \Gamma_{gl}\gamma_l\rangle \langle 0\chi_0\chi_1' a_l \Gamma_{gl}\gamma_l | V_{\Gamma_g\gamma_g} X_{\Gamma_g\gamma_g} | 0\chi_0\chi_0' \Gamma_{ge}\gamma_e\rangle}{(\mathcal{E}_{ui} - \mathcal{E}_f - \hbar\omega)(\mathcal{E}_{gl} - \mathcal{E}_e + \hbar\omega')}$$

$$+ \frac{\langle 1\chi_1\chi_1'\Gamma_{gf}\gamma_f | V_{\Gamma_g\gamma_g} X_{\Gamma_g\gamma_g} | 1\chi_1\chi_0' a_i \Gamma_{gi}\gamma_i\rangle \langle 1\chi_1\chi_0' a_i \Gamma_{gi}\gamma_i | P | 0\chi_1\chi_0' a_l \Gamma_{gl}\gamma_l\rangle \langle 0\chi_1\chi_0' a_l \Gamma_{ul}\gamma_l | V^{(n)}_{\Gamma_u\gamma_u} X^{(n)}_{\Gamma_u\gamma_u} | 0\chi_0\chi_0' \Gamma_{ge}\gamma_e\rangle}{(\mathcal{E}_{gi} - \mathcal{E}_f - \hbar\omega')(\mathcal{E}_{ul} - \mathcal{E}_e + \hbar\omega)}$$

$$+ \frac{\langle 1\chi_1\chi_1'\Gamma_{gf}\gamma_f | V^{(n)}_{\Gamma_u\gamma_u} X^{(n)}_{\Gamma_u\gamma_u} | 1\chi_0\chi_1' a_i \Gamma_{ui}\gamma_i\rangle \langle 1\chi_0\chi_1' a_i \Gamma_{ui}\gamma_i | V_{\Gamma_g\gamma_g} X_{\Gamma_g\gamma_g} | 1\chi_0\chi_0' a_l \Gamma_{ul}\gamma_l\rangle \langle 1\chi_0\chi_0' a_l \Gamma_{ul}\gamma_l | P | 0\chi_0\chi_0' \Gamma_{ge}\gamma_e\rangle}{(\mathcal{E}_{ui} - \mathcal{E}_f - \hbar\omega)(\mathcal{E}_{ul} - \mathcal{E}_f - \hbar\omega - \hbar\omega')}$$

$$+ \frac{\langle 1\chi_1\chi_1'\Gamma_{gf}\gamma_f | V_{\Gamma_g\gamma_g} X_{\Gamma_g\gamma_g} | 1\chi_1\chi_0' a_i \Gamma_{gi}\gamma_i\rangle \langle 1\chi_1\chi_0 a_i \Gamma_{gi}\gamma_i | V^{(n)}_{\Gamma_u\gamma_u} X^{(n)}_{\Gamma_u\gamma_u} | 1\chi_0\chi_0' a_l \Gamma_{ul}\gamma_l | P | 0\chi_0\chi_0' \Gamma_{ge}\gamma_e\rangle}{(\mathcal{E}_{gi} - \mathcal{E}_f - \hbar\omega')(\mathcal{E}_{ul} - \mathcal{E}_f - \hbar\omega - \hbar\omega')} \Bigg|^2$$

$$\times \delta(\mathcal{E}_f - \mathcal{E}_e + \hbar\nu + \hbar\omega' + \hbar\omega) \; . \tag{10}$$

To simplify the form of the two-phonon coupling, the following conditions are assumed:

(a) The electronic levels e and f are well isolated from neighboring levels, i.e., energy separation to nearest electronic states $\gg \hbar\omega'$.

(b) The odd-parity excited states i are sufficiently far above the electronic levels e and f such that

$$\hbar\omega \ll \mathcal{E}_{ui} - \mathcal{E}_f \simeq \mathcal{E}_{ui} - \mathcal{E}_e \simeq \Delta\mathcal{E}_{ui} \; . \tag{11}$$

In the case of the $\Gamma_{5g} \to \Gamma_{5g}$ transition, each electronic level involved is more than 1000 cm^{-1} from any neighboring level, thus satisfying condition (a). Condition (b) is reasonably well satisfied for d^8 electronic levels, as discussed in Paper I.

Where one of the two intermediate electronic states has even parity, because of condition (a) by far the largest contribution will arise when one of the electronic energies in the denominators cancel (i.e., when one of the intermediate electronic states is $\Gamma_{gf}\gamma_f'$ or $\Gamma_{ge}\gamma_e'$—one of the components of the ground or excited states). The contributions from other even electronic states will be neglected.

Where both of the intermediate states are of odd parity, the denominator is larger by a factor $\Delta\mathcal{E}_{ui}/\hbar\omega$ compared to the case where one of intermediate state is of even parity. Hence, terms in lines two and five of Eq. (10) can also be neglected.

Separating the electronic and vibrational parts, the transition probability of emitting a photon polarized in y direction with angular frequency between ν and $\nu + \Delta\omega$ into solid angle $\Delta\Omega$ is now given by

$$W_{e\to f}^{(2)} = \frac{\Delta\Omega\Delta\omega\nu^3 e^2}{2\pi c^3} \sum_{\gamma_e\gamma_f} \sum_{\substack{\vec{k},j \\ \vec{k}',j'}} \Bigg| \sum_{\substack{\Gamma_u\gamma_u n \\ \Gamma_g\gamma_g}} \Bigg[\sum_{\Gamma_{ui}\gamma_i a_i} \sum_{\gamma_e'} \Bigg(\frac{\langle \Gamma_{gf}\gamma_f | y | a_i\Gamma_{ui}\gamma_i\rangle \langle a_i\Gamma_{ui}\gamma_i | V^{(n)}_{\Gamma_u\gamma_u} | \Gamma_{ge}\gamma_e'\rangle \langle \Gamma_{ge}\gamma_e' | V_{\Gamma_g\gamma_g} | \Gamma_{ge}\gamma_e\rangle}{(\mathcal{E}_{ui}-\mathcal{E}_e)(\hbar\omega')}$$

$$+ \frac{\langle \Gamma_{gf}\gamma_f | V^{(n)}_{\Gamma_u\gamma_u} | a_i\Gamma_{ui}\gamma_i\rangle \langle a_i\Gamma_{ui}\gamma_i | y | \Gamma_{ge}\gamma_e'\rangle \langle \Gamma_{ge}\gamma_e' | V_{\Gamma_g\gamma_g} | \Gamma_{ge}\gamma_e\rangle}{(\mathcal{E}_{ui}-\mathcal{E}_f)(\hbar\omega')} \Bigg)$$

$$+ \sum_{\gamma_f'} \Bigg(\frac{\langle \Gamma_{gf}\gamma_f | V_{\Gamma_g\gamma_g} | \Gamma_{gf}\gamma_f'\rangle \langle \Gamma_{gf}\gamma_f' | y | a_i\Gamma_{ui}\gamma_i\rangle \langle a_i\Gamma_{ui}\gamma_i | V^{(n)}_{\Gamma_u\gamma_u} | \Gamma_{ge}\gamma_e\rangle}{(-\hbar\omega')(\mathcal{E}_{ui}-\mathcal{E}_e)}$$

$$+ \frac{\langle \Gamma_{gf}\gamma_f | V_{\Gamma_g\gamma_g} | \Gamma_{gf}\gamma_f'\rangle \langle \Gamma_{gf}\gamma_f' | V^{(n)}_{\Gamma_u\gamma_u} | a_i\Gamma_{ui}\gamma_i\rangle \langle a_i\Gamma_{ui}\gamma_i | y | \Gamma_{ge}\gamma_e\rangle}{(-\hbar\omega')(\mathcal{E}_{ui}-\mathcal{E}_f)} \Bigg)\Bigg]$$

$$\times \langle \chi_1 | X^{(n)}_{\Gamma_u\gamma_u} | \chi_0\rangle \langle \chi_1' | X_{\Gamma_g\gamma_g} | \chi_0'\rangle |^2 \, \delta(\mathcal{E}_f - \mathcal{E}_e + \hbar\nu + \hbar\omega' + \hbar\omega) \ . \qquad (12)$$

If the linear perturbation $V_{\Gamma_g\gamma_g}$ is diagonal, then the summation over the components of Γ_{ge} and Γ_{gf} can be replaced by $\gamma_f' = \gamma_f$ and $\gamma_e' = \gamma_e$. This will not apply in general, but is valid for the particular case of a Γ_{5g} level with an A_{1g} or E_g perturbation. This restriction is desirable in view of the simplification it gives.

The coupling parameter within the brackets becomes

$$\Bigg[\sum_{\Gamma_{ui}\gamma_i a_i} \Bigg(\frac{\langle \Gamma_{gf}\gamma_f | y | a_i\Gamma_{ui}\gamma_i\rangle \langle a_i\Gamma_{ui}\gamma_i | V^{(n)}_{\Gamma_u\gamma_u} | \Gamma_{ge}\gamma_e\rangle}{\mathcal{E}_{ui}-\mathcal{E}_e} + \frac{\langle \Gamma_{gf}\gamma_f | V^{(n)}_{\Gamma_u\gamma_u} | a_i\Gamma_{ui}\gamma_i\rangle \langle a_i\Gamma_{ui}\gamma_i | y | \Gamma_{ge}\gamma_e\rangle}{\mathcal{E}_{ui}-\mathcal{E}_f} \Bigg)\Bigg]$$

$$\times [\langle \Gamma_{ge}\gamma_e | V_{\Gamma_g\gamma_g} | \Gamma_{ge}\gamma_e\rangle - \langle \Gamma_{gf}\gamma_f | V_{\Gamma_g\gamma_g} | \Gamma_{gf}\gamma_f\rangle] \frac{1}{\hbar\omega'} \ . \qquad (13)$$

The first line is simply $F^{\gamma_e\to\gamma_f}_{y\Gamma_u\gamma_u n}$ defined earlier [Eq. (6)] and the second can be defined as

$$\Delta F^{\gamma_e\to\gamma_f}_{\Gamma_g\gamma_g} = \langle \Gamma_{ge}\gamma_e | V_{\Gamma_g\gamma_g} | \Gamma_{ge}\gamma_e\rangle - \langle \Gamma_{gf}\gamma_f | V_{\Gamma_g\gamma_g} | \Gamma_{gf}\gamma_f\rangle \ , \qquad (14)$$

and both of these are frequency independent, so that Eq. (12) reduces to

$$W_{e\to f}^{(2)} = \frac{\Delta\Omega\Delta\omega\nu^3 e^2}{2\pi c^3} \sum_{\gamma_e\gamma_f} \sum_{\substack{\Gamma_u\gamma_u n \\ \Gamma_g\gamma_g}} F^{\gamma_e\to\gamma_f}_{y\Gamma_u\gamma_u n} F^{\gamma_e\to\gamma_f *}_{y\Gamma_u\gamma_u n'} \Delta F_{\Gamma_g\gamma_g} \Delta F_{\Gamma_g\gamma_g}{}^* \sum_{\substack{\vec{k}j \\ \vec{k}j}} \langle \chi_1(\vec{k},j) | X^{(n)}_{\Gamma_u\gamma_u} | \chi_0(\vec{k},j)\rangle \langle \chi_0(\vec{k},j) | X^{(n)*}_{\Gamma_u\gamma_u} | \chi_1(\vec{k},j)\rangle$$

$$\times \left(\frac{1}{\hbar\omega(\vec{k},j)} \right)^2 \langle \chi_1(\vec{k},j') | X_{\Gamma_g\gamma_g} | \chi_0(\vec{k}',j')\rangle \langle \chi_0(\vec{k}',j') | X^*_{\Gamma_g\gamma_g} | \chi_1(\vec{k}',j')\rangle \, \delta(\mathcal{E}_f - \mathcal{E}_e + \hbar\nu + \hbar\omega(\vec{k},j) + \hbar\omega(\vec{k}',j')) \ , \qquad (15)$$

where the vibrational terms have been written in unabbreviated form. Expanding the vibrational terms by substituting for the symmetry displacement

$$X^{(n)}_{\Gamma_g} = \sum_{\vec{k}j} \mathcal{A}^{(n)}_{\Gamma\gamma}(\vec{k},j)\, q(\vec{k},j) \qquad (16)$$

and evaluating as for the one-phonon sideband gives

$$\sum_{\substack{\vec{k}j \\ \vec{k}'j'}} \frac{\hbar}{2\omega(\vec{k},j)} \mathcal{A}^{(n)}_{\Gamma_u\gamma_u} \mathcal{A}^{(n')}_{\Gamma_u\gamma_u}(\vec{k},j)^* \left(\frac{1}{\hbar\omega(\vec{k}',j')} \right)^2 \frac{\hbar}{2\omega(\vec{k}',j')} \mathcal{A}_{\Gamma_g\gamma_g}(\vec{k}',j') \mathcal{A}_{\Gamma_g\gamma_g}(\vec{k}',j')^* \, \delta(\hbar\omega(\vec{k},j) + \hbar\omega(\vec{k}',j') - \hbar\omega)$$

$$= \frac{1}{\hbar} \int \sum_{\vec{k}j} \frac{\hbar}{2\omega(\vec{k},j)} \mathcal{A}^{(n)}_{\Gamma_u\gamma_u} \mathcal{A}^{(n')}_{\Gamma_u\gamma_u}(\vec{k},j)^* \delta(\omega(\vec{k},j) - \omega_1)$$

$$\times \sum_{\vec{k}'j'} \left(\frac{1}{\hbar\omega(\vec{k}',j')} \right)^2 \frac{1}{2\omega(\vec{k}',j')} \mathcal{A}_{\Gamma_g\gamma_g}(\vec{k}',j') \mathcal{A}_{\Gamma_g\gamma_g}(\vec{k}',j')^* \delta(\omega(\vec{k}',j') + \omega_1 - \omega) \ . \qquad (17)$$

This can be reexpressed in terms of the continuous Green's function defined in Ref. 1,

$$\int_0^{\omega_{\max}} \frac{1}{\pi} \operatorname{Im} G_{\Gamma_u}^{(nn')}(\omega_1) \frac{1}{\hbar\pi} \frac{1}{(\omega-\omega_1)^2} \operatorname{Im} G_{\Gamma_g}(\omega-\omega_1)\, d\omega_1 \,. \tag{18}$$

Therefore, by defining

$$\mathcal{G}_{\Gamma_g}(\omega) = G_{\Gamma_g}(\omega)/\omega^2 \,, \tag{19}$$

the transition probability takes the final form

$$W_{e\to f}^{(2)} = W^{(2)}(\omega)\,\Delta\omega = \frac{\Delta\Omega\Delta\omega\nu^3 e^2}{2\pi c^3}$$

$$\times \sum_{\Gamma_u\gamma_u n n', \Gamma_g\gamma_g} \sum_{\gamma_e\gamma_f} F_{\gamma\Gamma_u\gamma_u n}^{\gamma_e\to\gamma_f} F_{\gamma\Gamma_u\gamma_u n'}^{\gamma_e\to\gamma_f *} \Delta F_{\Gamma_g\gamma_g}^{\gamma_e\to\gamma_f} \Delta F_{\Gamma_g\gamma_g}^{\gamma_e\to\gamma_f *}$$

$$\times \frac{1}{\hbar\pi} \int_0^{\omega_{\max}} \operatorname{Im} G_{\Gamma_u}^{(nn')}(\omega_1) \operatorname{Im} \mathcal{G}_{\Gamma_g}(\omega-\omega_1)\, d\omega_1 \,, \tag{20}$$

where $\omega_{\max}$ is the maximum frequency in the lattice.

The $\Delta F_{\Gamma_g\gamma_g}$ in this equation implies a difference in the force on the $\Gamma_g\gamma_g$ symmetry displacement between the ground and excited states. Such a force would result in a Jahn-Teller type of distortion (or a symmetrical A_{1g} expansion) of the nearest neighbors in at least one of the states. The component matrix elements of $\Delta F_{\Gamma_g\nu_g}$ are evaluated for the lattice in the defect equilibrium configuration, i.e., with the impurity ion in its ground state $f \equiv {}^3A_{2g}$, an orbital singlet, which shows no Jahn-Teller distortions. Therefore, all matrix elements associated with this state will be zero and the coupling coefficient related to the even mode reduces to

$$\Delta F_{\Gamma_g\gamma_g}^{\gamma_e\to\gamma_f} = \langle \Gamma_{ge}\gamma_e | V_{\Gamma_g\gamma_g} | \Gamma_{ge}\gamma_e \rangle \,, \tag{21}$$

and it is noted that for an A_{1g} or E_g perturbation,

$$\sum_{\gamma_g} \Delta F_{\Gamma_g\gamma_g}^{\gamma_e\to\gamma_f} \Delta F_{\Gamma_g\gamma_g}^{\gamma_e\to\gamma_f *} = \sum_{\gamma_g} \left| \langle \Gamma_{ge}\gamma_e | V_{\Gamma_g\gamma_g} | \Gamma_{ge}\gamma_e \rangle \right|^2 \tag{22}$$

$$= (\Delta F_{\Gamma_g})^2 \tag{23}$$

and is independent of γ_e (and γ_f). In this situation the transition probability takes on the simplified expression

$$W^{(2)}(\omega) = \sum_{\Gamma_g} (\Delta F_{\Gamma_g})^2 \int_0^{\omega_{\max}} \frac{\Delta\Omega\nu^3 e^2}{2\pi c^3}$$

$$\times \sum_{\Gamma_u nn'} \left[\sum_{\gamma_e\gamma_f} \sum_{\gamma_u} F_{\gamma\Gamma_u\gamma_u n}^{\gamma_e\to\gamma_f} F_{\gamma\Gamma_u\gamma_u n'}^{\gamma_e\to\gamma_f *} \right]$$

$$\times \frac{1}{\pi} \operatorname{Im} G_{\Gamma_u}^{(nn')}(\omega_1) \frac{1}{\hbar\pi} \operatorname{Im} \mathcal{G}_{\Gamma_g}(\omega-\omega_1)\, d\omega_1 \tag{24}$$

$$= \sum_{\Gamma_g} \frac{(\Delta F_{\Gamma_g})^2}{\hbar\pi} \int_0^{\omega_{\max}} W^{(1)}(\omega_1) \operatorname{Im} \mathcal{G}\,(\omega-\omega_1)\, d\omega_1 \,, \tag{25}$$

where $W^{(1)}(\omega_1)$ is the one-phonon distribution.

Attention will be restricted to where one even displacement predominates. The complex can always experience a radial relaxation of the lattice and hence a coupling to the A_{1g} Green's function. Also since the excited state $e \equiv {}^1T_{2g}$ is an orbital triplet it can be split by E_g or T_{2g} distortion. E_g is most probable since this involves radial motion rather than tangential motion of the neighbors.

The use of Born-Oppenheimer product wave functions in this particular case should still be justifiable in the presence of this distortion since the Jahn-Teller perturbation is diagonal and therefore the electronic states are not mixed by the nuclear motion. This situation has been summarized by Sturge.[7]

2. *Type* I: *Multiphonon*

The Jahn-Teller-type displacement will give rise to higher-order phonon processes arising from the same linear term in the perturbation. By extending the above treatment to r-phonon processes of which $(r-1)$ are even, the transition probability is given by

$$W^{(r)}(\omega) = \left[\frac{\Delta F_{\Gamma_g}}{\hbar\pi}\right]^{r-1} \frac{1}{(r-1)!}$$

$$\times \iint \cdots \int_0^{\omega_{\max}} d\omega_1 d\omega_2 \cdots d\omega_{r-1}\, W^{(1)}(\omega_1) \operatorname{Im} \mathcal{G}\,(\omega_2) \cdots \operatorname{Im} \mathcal{G}\,(\omega_{r-1}) \operatorname{Im} \mathcal{G}\,(\omega-\omega_1-\omega_2\cdots\omega_{r-1}) \tag{26}$$

$$= \frac{\Delta F_{\Gamma_g}}{\hbar\pi} \frac{1}{(r-1)} \int_0^{(r-1)\omega_{\max}} W^{(r-1)}(\omega_1) \operatorname{Im} \mathcal{G}_{\Gamma_g}(\omega-\omega_1)\, d\omega_1 \,. \tag{27}$$

We can see from this the standard result that the area under the r-phonon distribution varies as

$$\int_0^{r\omega_{\max}} W^{(r)}(\omega)\, d\omega = [S^{r-1}/(r-1)!] \int_0^{\omega_{\max}} W^{(1)}(\omega)\, d\omega \,, \tag{28}$$

where S is the ratio of the area under the two-phonon to the one-phonon intensity distribution,

$$S = \int_0^{2\omega_{\max}} W^{(2)}(\omega)\, d\omega \Big/ \int_0^{\omega_{\max}} W^{(1)}(\omega)\, d\omega \tag{29}$$

$$= \frac{\Delta F_{\Gamma_g}}{\hbar\pi} \int_0^{\omega_{\max}} \mathrm{Im}\mathcal{G}_{\Gamma_g}(\omega)\, d\omega \ . \tag{30}$$

Equation (30) relates S to the coupling parameter ΔF_{Γ_g}.

3. *Type* II: *Two Phonon*

Here it is assumed that there is no Jahn-Teller effect present and hence all matrix elements involving even-parity linear terms in the interaction potential will be zero. Then the quadratic term gives rise to a transition probability given by

$$W_{e\to f} = \frac{2\pi}{\hbar} \sum_{\gamma_e\gamma_f} \sum_{\text{final states}} \Bigg| \sum_{\Gamma_{ui}\gamma_i a_i} \Bigg(\frac{\langle 1\chi_1\chi_1'\Gamma_{gf}|P|0\chi_1\chi_1' a_i\Gamma_{ui}\gamma_i\rangle\langle 0\chi_1\chi_1' a_i\Gamma_{ui}\gamma_i|V_2|0\chi_0\chi_0'\Gamma_{ge}\gamma_e\rangle}{\mathcal{E}_{ui} - \mathcal{E}_e + \hbar\omega + \hbar\omega'}$$

$$+ \frac{\langle 1\chi_1\chi_1'\Gamma_{gf}\gamma_f|V_2|1\chi_0\chi_0' a_i\Gamma_{ui}\gamma_i\rangle\langle 1\chi_0\chi_0' a_i\Gamma_{ui}\gamma_i|P|0\chi_0\chi_0'\Gamma_{ge}\gamma_e\rangle}{\mathcal{E}_{ui} - \mathcal{E}_f - \hbar\omega - \hbar\omega'} \Bigg) \Bigg|^2 \delta(\mathcal{E}_f - \mathcal{E}_e + \hbar\nu + \hbar\omega + \hbar\omega') \ . \tag{31}$$

This reduces in a manner similar to the one-phonon sideband to give

$$W_{e\to f} = W^{(2)}(\omega)\,\Delta\omega = \frac{\Delta\Omega\Delta\omega\nu^3 e^2}{2\pi c^3} \sum_{\Gamma_g\Gamma_u nn'} \Bigg(\sum_{\gamma_e\gamma_f} \sum_{\gamma_u\gamma_g} F^{\gamma_e\to\gamma_f}_{y\Gamma_u\gamma_u n,\Gamma_g\gamma_g} F^{\gamma_e\to\gamma_f *}_{y\Gamma_u\gamma_u n',\Gamma_g\gamma_g} \Bigg) \int_0^{\omega_{\max}} \mathrm{Im}G^{(nn')}_{\Gamma_u}(\omega_1)\, \mathrm{Im}G_{\Gamma_g}(\omega-\omega_1)\, d\omega_1 \ , \tag{32}$$

where

$$F^{\gamma_e\to\gamma_f}_{y\Gamma_u\gamma_u n,\Gamma_g\gamma_g} = \sum_{\Gamma_{ui}\gamma_i a_i} \Bigg(\frac{\langle\Gamma_{gf}\gamma_f|y|a_i\Gamma_{ui}\gamma_i\rangle\langle a_i\Gamma_{ui}\gamma_i|V^{(n)}_{\Gamma_u\gamma_u,\Gamma_g\gamma_g}|\Gamma_{ge}\gamma_e\rangle}{(\mathcal{E}_{ui} - \mathcal{E}_e)}$$

$$+ \frac{\langle\Gamma_{gf}\gamma_f|V^{(n)}_{\Gamma_u\gamma_u,\Gamma_g\gamma_g}|a_i\Gamma_{ui}\gamma_i\rangle\langle a_i\Gamma_{ui}\gamma_i|y|\Gamma_{ge}\gamma_e\rangle}{(\mathcal{E}_{ui} - \mathcal{E}_f)} \Bigg) \ . \tag{33}$$

Note in this coupling mechanism that the functional form of the distribution coupled differs by a factor ω^2 compared to coupling type I.

4. *Type* II: *Multiphonon*

If the above was the predominant two-phonon coupling mechanism, then the likely three-phonon coupling would arise from the third term V_3 in the expansion of the electron-phonon interaction, the r-phonon process from the V_r term in the expansion. It is noted in this case that (i) the coupling parameters are not simply related to one another and (ii) odd-symmetry-displacement types can also be coupled.

In the calculation which follows, it will be assumed that coupling of one particular even-symmetry displacement will give by far the largest coupling, however, it is clear from the above that it is difficult to justify such an assumption in this coupling type.

V. GREEN'S FUNCTIONS

In Paper I, details of a numerical calculation of odd-parity imperfect-lattice Green's functions have been presented. Here the four even-parity functions are required in addition and, therefore, calculations are extended to include these cases. The method of calculation of the perfect-lattice functions are identical and the results are shown by the solid curve in Figs. 3–6.

The imperfect-lattice response functions are related to the above by[1]

$$\underline{G}^{\mathrm{imp}}(\omega) = [\underline{I} + \underline{G}(\omega)\,\underline{\Delta K}(\omega)]^{-1}\,\underline{G}(\omega) \ , \tag{34}$$

where $\underline{\Delta K} = \Delta A$, the longitudinal force constant change in the case of the A_{1g} and E_g response functions, and $\underline{\Delta K} = \Delta B$, the transverse force constant in the case of T_{1g} and T_{2g}. The imaginary parts of the Green's functions are shown for two possible force-constant changes by the dashed curves in the same Figs. 3–6.

VI. COMPARISON WITH EXPERIMENT FOR $\Gamma_{5g} \to \Gamma_{5g}$ TRANSITION

The one-phonon process is necessarily of odd parity and, if it gives rise to the peaks at 205 and 398 cm^{-1}, the distribution makes excellent comparison both in shape and positions to the response function where allowance is made for the changed mass and a small softening $\Delta A = -8\ \mathrm{N/m}^2$ of the force constant A. (Compare experiment with Fig. 7 of Ref. 1.)

Further phonons can couple to the transition by either of the mechanisms treated in Sec. IV. For

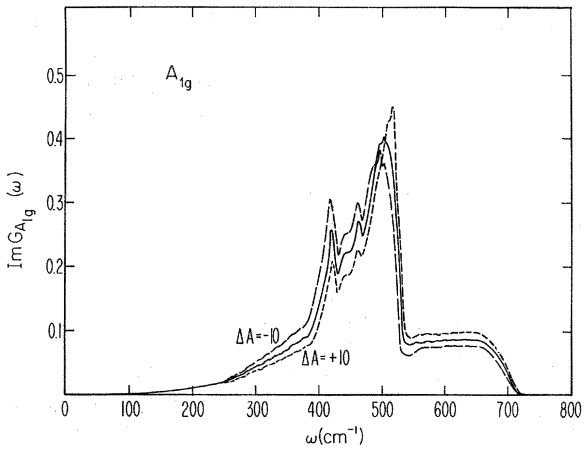

FIG. 3. Imaginary part of the A_{1g} Green's function. The solid curve gives the perfect-lattice Green's function, whereas the dashed curves give the functions where changes ΔA in N/m have been made in the longitudinal A force constant. The vertical scale is in units of 10^{-28} $\mathrm{sec}^2/\mathrm{amu}$.

type I, the sideband takes on a simple form (27) with only one additional parameter for each even displacement. The form for type II is far more complex and there are too many parameters to consider them all empirically and unrelated. Therefore, to make some calculation in this case it will be assumed that the area under the rth phonon process again obeys Eq. (28), i.e., imposing a relation between the parameters of various orders.

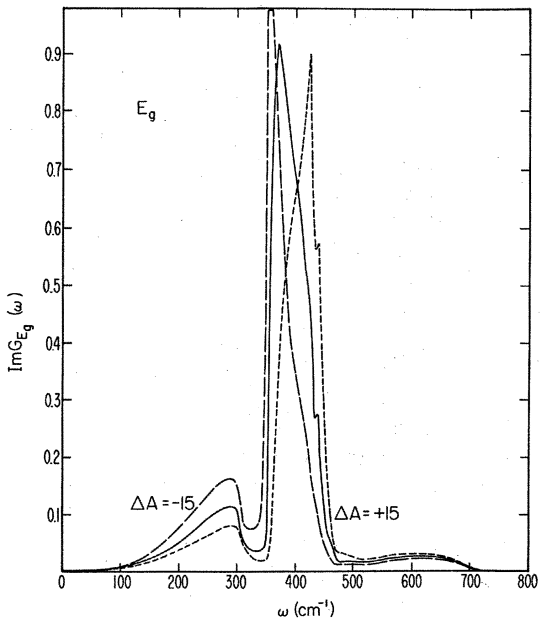

FIG. 4. Imaginary part of the E_g Green's function. Notation and units same as in Fig. 3.

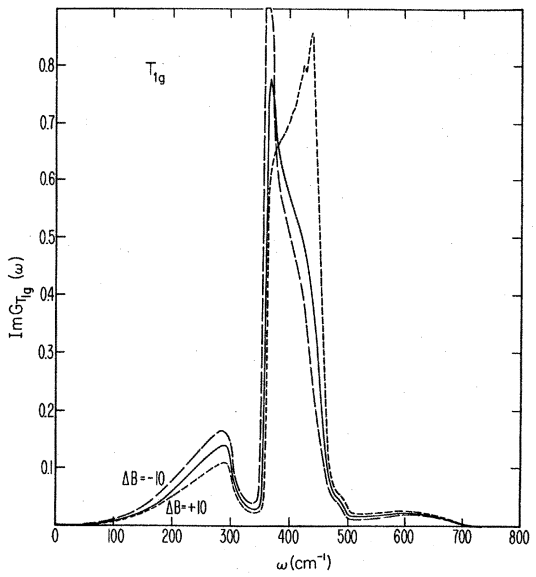

FIG. 5. Imaginary part of the T_{1g} Green's functions. The solid curve gives the perfect-lattice Green's function and the dashed curves give the functions where changes ΔB in N/m have been made in the transverse force constant B. The vertical scale is in units of 10^{-28} $\mathrm{sec}^2/\mathrm{amu}$.

For both coupling mechanisms the simplified case in which one even symmetry displacement is predominant will be calculated. The results do not merit extending the calculation to any more general a case. This is the most likely situation if the coupling arises from a Jahn-Teller type of distortion, i.e., type I, perhaps less likely in the case of type II as remarked earlier.

Then the form of the r-phonon distribution is given in both cases by

$$W^{(r)}(\omega) = \int\int\cdots\int_0^{\omega_{\max}} d\omega_1\, d\omega_2 \cdots d\omega_{r-1}\, W^{(1)}(\omega_1)$$

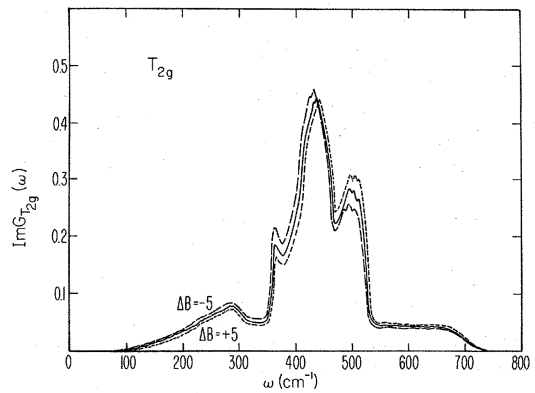

FIG. 6. Imaginary part of the T_{2g} functions. Notation and units as for Fig. 5.

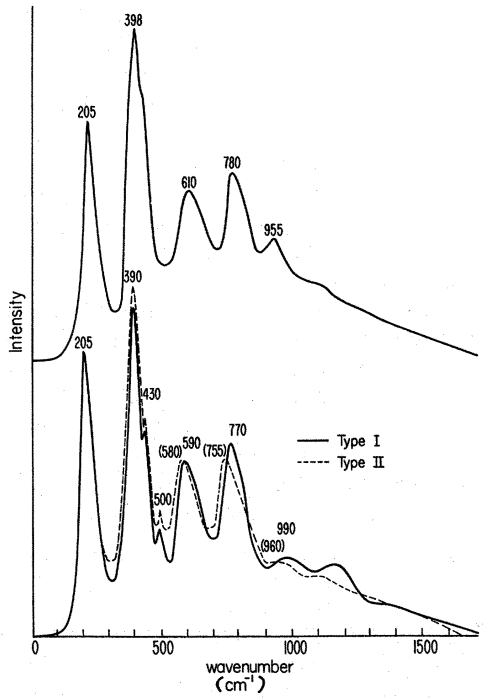

FIG. 7. Comparison of constructed band and experiment. The top curve is the experimental spectrum. The lower traces are the theoretical constructions using up to four phonons. The first phonon band (odd parity) giving the first two peaks is given by the $G^{(11)}_{T_{1u}}(\omega)$ response function. Higher phonon processes involve the coupling of $G_{E_g}(\omega)/\omega^2$ (type I) or $G_{E_g}(\omega)$ (type II) response function with the parameter $S=1$. (All response functions are for defect lattice; $\Delta m = 34.39$ amu, $\Delta A = -8$ N/m, $\Delta B = 0$.)

$$\times \mathrm{Im}\bar{G}_{\Gamma_g}(\omega_2)\cdots \mathrm{Im}\bar{G}_{\Gamma_g}(\omega-\omega_1-\omega_2\cdots-\omega_{r-1}) \,, \quad (35)$$

where $W^{(1)}(\omega_1)$ is the first odd-phonon distribution,

$$\bar{G}_{\Gamma_g}(\omega) = \mathcal{G}_{\Gamma_g}(\omega) = G_{\Gamma_g}(\omega)/\omega^2 \text{ for coupling type I} \,, \quad (36)$$

$$\bar{G}_{\Gamma_g}(\omega) = G_{\Gamma_g}(\omega) \quad \text{for coupling type II,} \quad (37)$$

the coupled mode being Γ_g.

These distributions (35) are evaluated for up to four-phonon processes weighted according to Eq. (28) and added to give the curves in Figs. 7 and 8 for coupling to A_{1g} and to E_g displacements. The response functions adopted correspond to a mass change $\Delta m = 34.39$ amu and force-constant changes $\Delta A = -8$ N/m and $\Delta B = 0$. The ΔF_g parameter is adjusted to give the ratio of the area under the first phonon distribution to the area under the second phonon distribution to be equal (i.e., $S=1$).

It can be seen from these figures that the agreement using coupling to E_g vibrations is excellent for general shape and peak positions, whereas the agreement is poor in the case of the A_{1g} vibrations. The difference between the curves for coupling types I and II is small and the comparison between experiment and the alternative constructions (Fig. 7) only marginally favor type II. It is anticipated, however, that for type-II coupling A_{1g} would predominate as the coupling parameters will be larger. A_{1g} introduces an additional monopole term within the coupling matrix element, whereas E_g would introduce at best octopole terms (similarly, T_{1g} and T_{2g} would be smaller than A_{1g}). Thus, the strong E_g coupling suggests that a Jahn-Teller distortion and a coupling of type I is the more likely explanation. The excited state is orbitally T_{2g} and quite possibly, as discussed earlier, experiences such an E_g distortion[7]; however, it has not been possible at present to substantiate this from any other experimental data.

VII. $\Gamma_{3g}-\Gamma_{5g}$ TRANSITION

Good agreement is obtained for the one-phonon sideband using the following admixture of Green's functions as given in Paper I:

$$\mathrm{Im}G^{(11)}_{T_{1u}}(\omega) + 0.025\,\mathrm{Im}G^{(22)}_{T_{1u}} + 0.25\,\mathrm{Im}G^{(12)}_{T_{1u}}(\omega) \,. \quad (38)$$

The imperfect-lattice functions corresponded to the

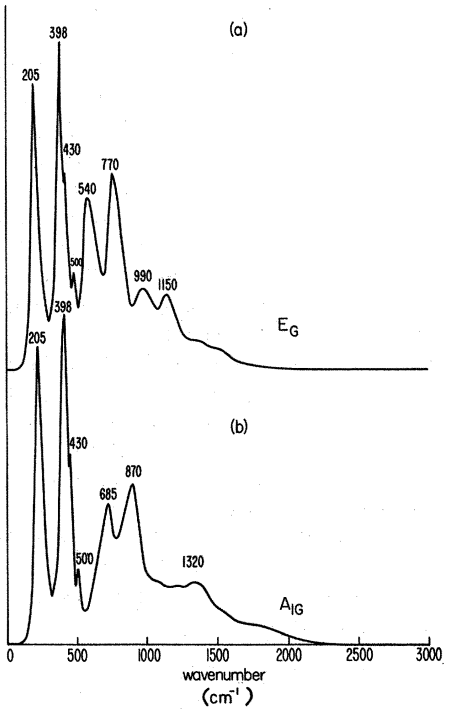

FIG. 8. Comparison of constructed bands for coupling (type I) in second- and higher-order processes using (a) $G_{E_g}(\omega)$ and (b) $G_{A_g}(\omega)$ response functions. E_g corresponds to type I in Fig. 7 and the empirical parameters are the same.

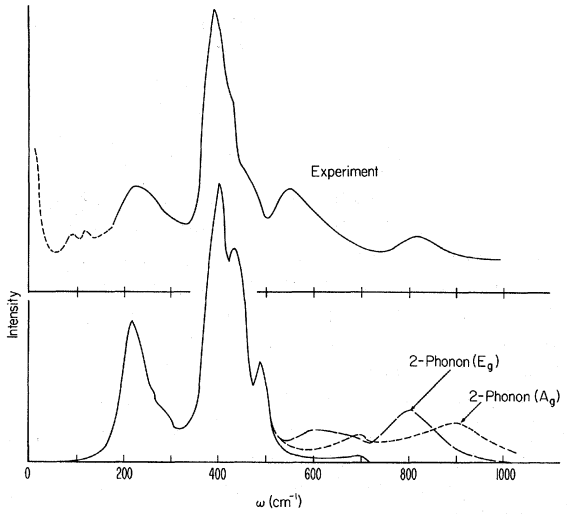

FIG. 9. Comparison between the vibronic emission band of the Ni^{2+} $\Gamma_{3g}(^3T_{2g}, t_{2g}^5 e_g^3)$-$\Gamma_{5g}(^3A_{1g}, t_{2g}^6 e_g^2)$ transition and the empirical Green's-function construction of the band including two-phonon process. The one-phonon construction is given in Eq. (3); the two-phonon process includes additional coupling to E_g or A_{1g} functions. The Green's functions used are those for the imperfect MgO lattice with allowance made for the mass change but no force-constant changes.

substitution of the mass of a Ni^{2+} ion but no changes in force constants.

The two-phonon distributions calculated for this transition in a manner similar to the above treatment of the $\Gamma_{5g}(^1T_{2g}, t_{2g}^5 e_g^3)$-$\Gamma_{5g}(^3A_{2g}, t_{2g}^6 e_g^2)$ transition are shown in Fig. 9 for the coupling to E_g and A_{1g} displacements. The traces are those for type-II coupling; however, these are very similar to those for type-I coupling. The peak at 540 cm^{-1} is thought to be a one-phonon peak[1] and, therefore, it can be seen that there is again fair agreement with the two-phonon vibronic band assuming coupling to the E_g vibration, although the strength of the coupling itself is much weaker. The applicability of the model to this transition is doubtful. This is because there are other electronic energy levels within the range of lattice vibrations (i.e., other spin-orbit levels of the $^3T_{2g}$ state), and therefore condition (a) of Sec. IV is not satisfied. A coupling to the E_g function possibly implies in this instance that these electronic states are being coupled by E_g vibrations.

VIII. COMPARISON BETWEEN THE TWO TRANSITIONS

It is worth commenting on the use of different effective force constants for the two transitions $\Gamma_{3g}(^3T_{2g}, t_{2g}^5 e_g^3)$-$\Gamma_{5g}(^3A_{2g}, t_{2g}^6 e_g^2)$ and $\Gamma_{5g}(^1T_{2g}, t_{2g}^5 e_g^3)$-$\Gamma_{5g}(^3A_{2g}, t_{2g}^6 e_g^2)$. Clearly, there are really different force constants associated with each level of the Ni^{2+} ion. However, the variation of the force constants is only a few percent (~ 5%) and this amount of change does not give rise to shifts in the peak positions of the response functions by greater than 20 cm^{-1} or substantial changes in their characteristic shapes (see Figs. 3–6). Thus the use of effective force constants for a transition should be fair and certainly should not give rise to misinterpretation of which displacements are coupling to each transition.

Note that changing the force constants between ground and excited states can also give rise to additional coupling. However, the force constants changed and the relaxation of the lattice (Jahn-Teller or symmetrical expansion) are interrelated and will couple the same displacement type. This will be allowed for when the coupling parameters are treated empirically as done here.

IX. ONE-PHONON COUPLING PARAMETERS

The one-phonon coupling parameters for the $\Gamma_{5g}(^1T_{2g}, t_{2g}^5 e_g^3)$-$\Gamma_{5g}(^3A_{2g}, t_{2g}^6 e_g^2)$ transition were calculated using the same assumptions made in Ref. 1, i.e., considering the effect of the varying electric field at the participating electron due to the motion of the nearest neighbors (considered as point charges). Again, all intermediate states are assumed to be at the same energy level so that closure may be used.

The transition is only permitted by spin-orbit coupling, and therefore there are no coupling parameters in the strong-field limit. Using the eigenstates obtained from diagonalizing Liehr and Ballhausen energy matrices [Ref. 4, Eq. (4)] for parameters given in Sec. IV, the coupling parameters give the following linear combination of Green's functions:

$$\mathrm{Im}G_{T_{1u}}^{(11)}(\omega) + 5.42\,\mathrm{Im}G_{T_{1u}}^{(22)}(\omega) + 3.28\,\mathrm{Im}G_{T_{1u}}^{(12)}(\omega) + 1.02\,\mathrm{Im}G_{T_{2u}}(\omega)\ . \quad (39)$$

These do not agree with the empirical parameters where the coupling is totally to the $G_{T_{1u}}^{(11)}(\omega)$ response function and this conclusion is not changed if the spin-orbit coupling parameter is altered by 20%.

The model is crude but had given good agreement for the Ni^{2+} $\Gamma_{3g}(^3T_{2g}, t_{2g}^5 e_g^3)$-$\Gamma_{5g}(^3A_{2g}, t_{2g}^6 e_g^2)$ transition[1,8] and the V^{2+}, ^2E_g-^4A_g transition.[8] The breakdown of the agreement in this case is not understood.

X. CONCLUSIONS

A model which assumes the predominant perturbation arises from the interaction with the nearest neighbors is again used with marked success. The initial one-phonon part of the band is

well fitted by the imperfect-lattice $G^{(11)}_{T_{1u}}(\omega)$ response function with only small percentage changes in the lattice force constants. The multiphonon region can be constructed with successive coupling to the $G_{E_g}(\omega)$ response function. This could easily be understood if there were an E_g Jahn-Teller distortion in the excited state. However, there is another coupling mechanism which could explain this coupling and it has not been possible to conclusively establish the presence of such a Jahn-Teller distortion.

The crude point-charge calculation of one-phonon coupling which was used successfully for previous transitions of impurities in MgO has been used without success—placing some doubt on the validity of such a model.

ACKNOWLEDGMENTS

I would like to acknowledge the advice and encouragement of Dr. R. W. H. Stevenson, and Professor C. McCombie and Dr. M. J. Sangster for the use of their computer calculation of Green's functions. Thanks also to my colleagues for many useful discussions.

†Research conducted at University of Aberdeen supported by the Science Research Council and at UCLA supported by U. S. Army Research Office, Durham, N.C.

*Now at Queen Mary College, London, England.

[1]N. B. Manson, preceding paper, Phys. Rev. B 4, 2645 (1971).

[2]J. E. Ralph and M. G. Townsend, J. Phys. C 3, 8 (1970).

[3]J. E. Ralph and M. G. Townsend, J. Chem. Phys. 48, 149 (1968).

[4]A. D. Liehr and C. J. Ballhausen, Am. J. Phys. (N.Y.) 6, 134 (1959).

[5]H. A. Jahn and E. Teller, Proc. Phys. Soc. (London) A161, 220 (1937).

[6]M. D. Sturge suggested for similar transition in MgO: Ni^{2+} in Ref. 7, p. 184.

[7]M. D. Sturge, in *Solid State Physics*, edited by F. Seitz and D. Turnbull (Academic, New York, 1967), Vol. 20, p. 91.

[8]M. J. L. Sangster and C. W. McCombie, J. Phys. C 3, 1498 (1970).

PHYSICAL REVIEW B VOLUME 4, NUMBER 8 15 OCTOBER 1971

Vibronic Structure and Optical Properties of the $M(C_{2h})$ Center in MgF_2 †

M. Mostoller, B. Henderson,* W. A. Sibley,‡ and R. F. Wood
Solid State Division, Oak Ridge National Laboratory, Oak Ridge, Tennessee 37830
(Received 10 March 1971)

The optical properties of the $M(C_{2h})$ center in MgF_2 are analyzed in terms of an effective one-phonon density of states, using a combination of convolution integration and moment analysis. A satisfactory fit to the experimental absorption spectrum at $T=0$ is obtained for this intermediate coupling case, including particularly the sharp structure seen in the one-phonon region. Good agreement between theory and experiment is also found for the no-phonon line and broad-band parameters in absorption as functions of temperature. A calculated luminescence spectrum, derived from that for absorption by using a simple model to estimate the quadratic coupling, compares well with the observed emission band at $T=0$.

I. INTRODUCTION

A practical procedure for calculating the optical absorption and emission spectra of impurities in insulators was described in a recent paper by Mostoller, Ganguly, and Wood[1] (referred to hereafter as MGW). The computational approach was based on the well-known theory of optical processes associated with such impurities. It provided for (i) an iterative scheme for finding an effective one-phonon density of states; (ii) the convolution of this one-phonon spectrum to find the contributions of the n-phonon processes in those regions where vibronic structure occurs; (iii) the use of moment analysis for higher n-phonon processes which do not contribute discernible structure; (iv) the retention of the lowest-order effects of quadratic coupling on the temperature dependence of the zero-phonon line's half-width and peak position; (v) a simple transformation between phonon operators in the ground and excited electronic states of the impurity which breaks the mirror symmetry between the absorption and emission spectra characteristic of the linear coupling approximation. As an illustrative example, the absorption spectrum of the N_1 center in NaCl was chosen because it exhibits a great deal of phonon structure. However, little is known about either its emission spectrum (if it exists) or the temperature dependence of its zero-phonon line, so that some aspects of the computational approach could not be tested.